PROCEEDINGS OF THE ROYAL SOCIETY B

Proc. R. Soc. B (2009) **276**, 3747–3752
doi:10.1098/rspb.2009.1003
Published online 5 August 2009

Lift production in the hovering hummingbird

Douglas R. Warrick[1,*], Bret W. Tobalske[2] and Donald R. Powers[3]

[1]*Department of Zoology, Oregon State University, 3029 Cordley Hall, Corvallis, OR 97331, USA*
[2]*Field Research Station at Fort Missoula, Division of Biological Sciences, University of Montana, Missoula, MT 59812, USA*
[3]*Biology Department, George Fox University, 414 N. Meridian Street, Newberg, OR 97132, USA*

Aerodynamic theory and empirical observations of animals flying at similar Reynolds numbers (*Re*) predict that airflow over hummingbird wings will be dominated by a stable, attached leading edge vortex (LEV). In insects exhibiting similar kinematics, when the translational movement of the wing ceases (as at the end of the downstroke), the LEV is shed and lift production decreases until the energy of the LEV is re-captured in the subsequent half-cycle translation. We here show that while the hummingbird wing is strongly influenced by similar sharp-leading-edge aerodynamics, leading edge vorticity is inconsistent, varying from 0.7 to 26 per cent (mean 16%) of total lift production, is always generated within 3 mm of the dorsal surface of the wing, showing no retrograde (trailing to leading edge) flow, and does not increase from proximal to distal wing as would be expected with a conical vortex (class III LEV) described for hawkmoths. Further, the bound circulation is not shed as a vortex at the end of translation, but instead remains attached and persists after translation has ceased, augmented by the rotation (pronation, supination) of the wing that occurs between the wing-translation half-cycles. The result is a near-continuous lift production through wing turn-around, previously unknown in vertebrates, able to contribute to weight support as well as stability and control during hovering. Selection for a planform suited to creating this unique flow and nearly-uninterrupted lift production throughout the wingbeat cycle may help explain the relatively narrow hummingbird wing.

Keywords: aerodynamics; hummingbirds; flight

1. INTRODUCTION

Small animals flying at low *Re* numbers (<5000) have been shown to employ aerodynamic mechanisms different from larger animals or machines. The results of dynamic robotic simulations of insects such as fruit flies ($Re = 120$) and hawkmoths ($Re = 5000$) have shown that these animals present their wings at high angles of attack, generate conditions of dynamic stall over their wings, and are thereby capable of generating lift coefficients higher than those resulting from low angle of attack and more typical laminar flow over larger aerofoils (Ellington *et al.* 1996; Willmott *et al.* 1997; Dickinson *et al.* 1999; Bomphrey *et al.* 2005, 2006). These studies also show that some insects employ wing rotation to generate lift during wing turn-around (Dickinson *et al.* 1999), and that the circulation of the leading edge vortex (LEV), shed at the end of the wing half-cycle, can be re-captured in the subsequent reversing half cycle. The flow characteristics over this *Re* range include the establishment of a stable LEV over the upper surface of the wing that flows axially away from the wing root and merges into the tip vortex wake (Willmott *et al.* 1997) or may be continuous over the dorsal body of the insect (Bomphrey *et al.* 2005). In any case, key to the use of LEVs as lift mechanisms is that they are stable enough to remain attached to the wing for the period of wing translation, rather than be shed into the wake, as is the case when a more typical aerofoil loses lift after it stalls. It has been suggested that persistent LEVs are made possible by the intrinsically more stable flows at low *Re* numbers, and that this mechanism may therefore be available to only small fliers (Birch *et al.* 2004; Lehmann 2004; Ellington 2006).

While employing wing kinematics during hovering strikingly similar to those of insects (Weis-Fogh 1972; Tobalske *et al.* 2007), hummingbirds present their wings at lower angles of attack (Tobalske *et al.* 2007) and operate at sufficiently high *Re* numbers ($Re \approx 7000$; using a wingtip speed of 14 m s^{-1} and an average wing chord of 0.01 m as characteristic length) that it is unclear whether the flow characteristics over their wings should be similar to that of insects, although a recent study of bats flying at similar *Re* showed that larger fliers may also take advantage of leading edge vorticity (Muijres *et al.* 2008). Further, although the long-axis wing rotation between the half-cycles of hummingbirds has been shown to produce useful aerodynamic force in robotic simulations of insect flight, the aerodynamic properties of this phase of the wing cycle have never been documented in a hummingbird, or any live animal. We hypothesized that both LEVs and rotational circulation mechanisms could be available to hummingbirds, being intermediate in size and mass to insects and bats and other birds. We here use particle image velocimetry (PIV) to observe the cross-sectional (two-dimensional) flow characteristics over the wings of hovering hummingbirds throughout the wingbeat cycle (electronic supplementary material, figure 1).

* Author for correspondence (warrickd@science.oregonstate.edu).

Electronic supplementary material is available at http://dx.doi.org/10.1098/rspb.2009.1003 or via http://rspb.royalsocietypublishing.org.

Received 10 June 2009
Accepted 16 July 2009

2. MATERIAL AND METHODS

(a) *Particle image velocimetry*

We sampled the near-field (1–50 mm from the surface of the wing) flow over the wings of rufous hummingbirds (*Selasphorus rufus*, $n = 7$; mean ± s.d. mass = 3.3 ± 0.1 g) as they hovered in a bottomless 60 × 60 × 85 cm Plexiglas cube. The birds were trained to fly to a feeder (1 ml syringe containing a 20% sucrose solution), the placement of which was manipulated to allow two-dimensional sampling of four chord sections at 1 cm intervals, from 2 cm from the wing root to the wingtip during downstroke and from 3 cm to the wingtip during upstroke. Our PIV system is manufactured by LaVision Inc, with recording and analysis accomplished using DaVis (v. 7.1). We used a dual cavity pulsed 50 mJ ND:YAG laser to illuminate a flow field of approximately 3 mm thick, with planar dimensions spanning from 5 cm above to 5 cm below the wing. The air was seeded with submicron-sized particles of olive oil vapour, generated using a Laskin nozzle at a rate of 7×10^{10} particles s^{-1}. Particle illumination was recorded using a 1376 × 1040 pixel CCD camera. To calculate velocity, a cross-correlation with adaptive multipass was employed; this method correlates within areas beginning at 64 × 64 pixel and decreasing to 16 × 16 pixel with 50 per cent overlap. For some images, a sliding background (scale length, 2 pixels) was used to subtract feather reflection from the raw image. A correlation peak error of 0.1 pixel, and average particle separation in the wake of 12 pixels, produced 1 per cent; error (Raffel *et al.* 2002; Spedding *et al.* 2003*a*,*b*); combined with optical distortion and particle–fluid fidelity error, our observed measurement error is 2.3 ± 0.5% (Raffel *et al.* 2002). Simultaneous digital video (500 fps; Photron PCI 1024), taken from directly above the bird, allowed synchronization of PIV images with wing kinematics.

(b) *Circulation and weight support*

We calculated circulation (Γ, $m^2\,s^{-1}$) from planar flow field images ($n = 120$) at 1 cm intervals from the wing root to the tip (figure 1*a*,*b*; electronic supplementary material, figure 2). Circulation, representing the strength of the lift-producing vortex created by translational wing movement, was calculated as line integral of velocity along a closed-loop, circular profile through the flow field around the aerofoil chord section (figure 1*a*,*b*; Finnemore & Franzini 2003):

$$\Gamma_{\text{bound}} = \oint V_{xy}\, \mathrm{d}l\, \cos\theta,$$

where dl is the path segment length, θ is the difference between the direction and the airflow direction in the xy plane and V_{xy} is the velocity of the airflow in the xy plane. We present data from the most thoroughly sampled 4 cm wing section, which showed greatest mean circulation of the span sections (electronic supplementary material, figure 2). Within a given reference frame, the direction of downstroke circulation was opposite to that of upstroke—that is, if the calculated downstroke circulation was positive, the calculated upstroke circulation was negative. The sign of circulation is nothing more than a result of an arbitrary reference frame, and we henceforth omit it, presenting circulation data as absolute values, so that the trends in strength of circulation are comparable between the half-strokes. Three velocity profiles for both the x and y dimensions (V_x, V_y) were taken along a circular path around the chord of the wing for each image, varying the distance from the wing to ensure that no profiles were too far away to adequately sample the energy

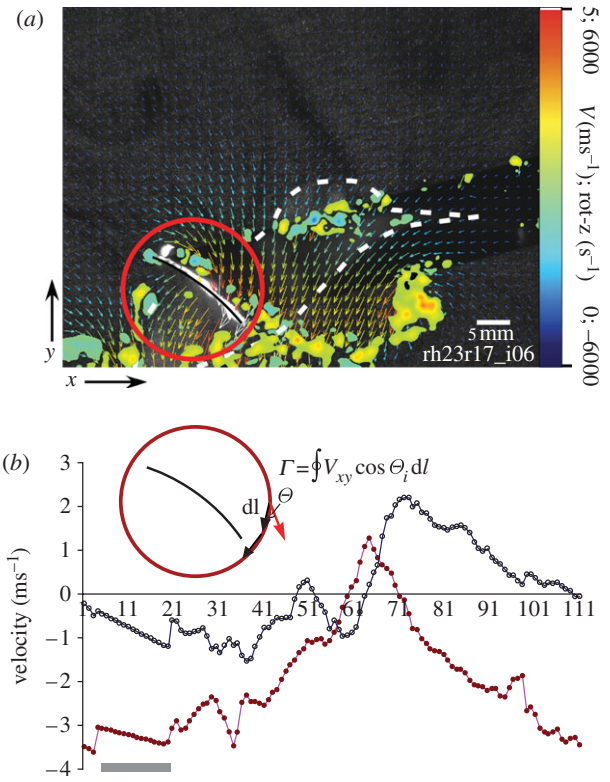

Figure 1. (*a*) Example of an x-sectional two-dimensional flow field around the wing (black line highlights chord x-section) 4 cm from the wing root of a hovering hummingbird at mid-upstroke (wing position 6; figure 4). The red circle is the profile path around the wing from which circulation was calculated. (*b*) Velocity data (V_x, V_y) from the above profile, and the calculation of circulation (Γ_{bound}); here $|\Gamma_{\text{bound}}| = 0.05\ m^2 s^{-1}$. Portions of the velocity profiles above the grey line (here, 8% of the profile) were linear interpolations replacing anomalous/absent vectors resulting from the wing shadow preventing accurate particle tracking. Dorsal vorticity is not reported for this image owing to the shadow effects on vector calculation (note spurious vectors and vorticity from poorly tracked particles in the wing shadow forward of the bird. In subsequent images, this vorticity is deleted from the image). Colour bars refer to both the range of vorticity and velocity of air (i.e. vector arrows). Open circles, V_x; filled circles, V_y.

of circulation. Mean ($n = 120$) coefficient of variation (s.d. mean^{-1}) between the three profiles within an image was 8 per cent.

In the distal wing, feathers were translucent to laser light, allowing near-complete illumination and description of the flow field around the wing chord. In images where shadows obscured portions (average ± s.d. = 13.6 ± 7% of the profile) of the vector field, especially in the more proximal wing, linear interpolation was used to fill velocity values (figure 1*b*). We limited our analysis to views where the chord of the wing was parallel to the camera and laser plane. We tested whether observed Γ_{bound} was sufficient to support the body weight by comparing Γ_{bound} to circulation required (Γ_o) = $WT/\rho S$, where W is body weight (in N), T is time per wingbeat (in s), ρ is air density and S is the projected horizontal area (in m^2) swept by the two wings (Spedding *et al.* 2003*a*,*b*).

We also computed the strength of the vorticity (ω, s^{-1}) on the upper surface of the wing—the so-called LEV, from post-processed vector fields using a median filter, then computing rot z[dy/dx]. Background ω, measured 2–3 cm outside the

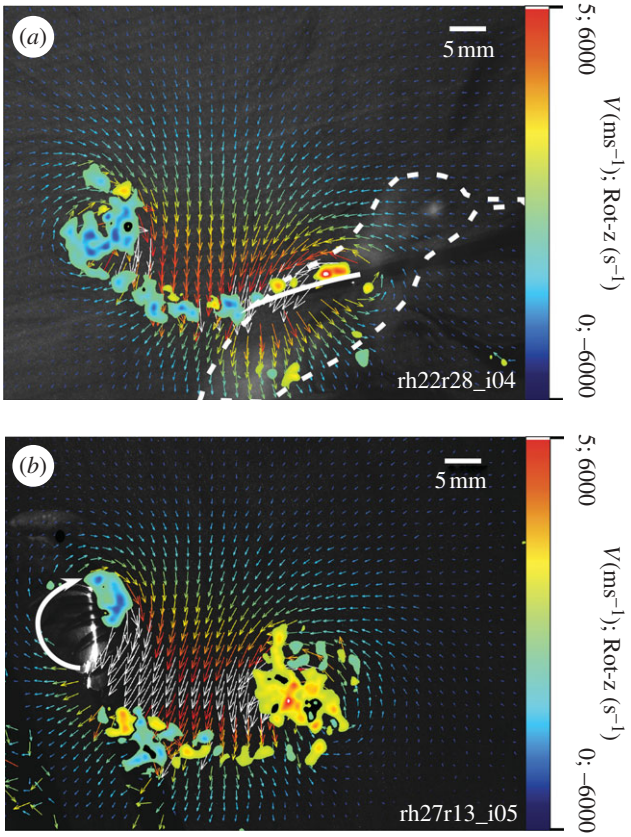

Figure 2. (*a*) Two-dimensional flow field around the wing (4 cm *x*-section) of a hovering hummingbird during mid-downstroke (wing position 2; figure 4). Much of the vorticity (positive anticlockwise rotation in red; negative clockwise in blue) over the dorsal surface is a result of boundary layer shear within 2 mm of the wing; circulation from the sum of this vorticity is 6 per cent of the bound circulation ($|\Gamma_{\text{bound}}| = 0.11\ \text{m}^2\ \text{s}^{-1}$) around the wing. (*b*) Flow during supinating rotation (large white arrow; wing position 4). The dorsal vorticity in this image is 26 per cent of the bound circulation ($|\Gamma_{\text{bound}}| = 0.15$).

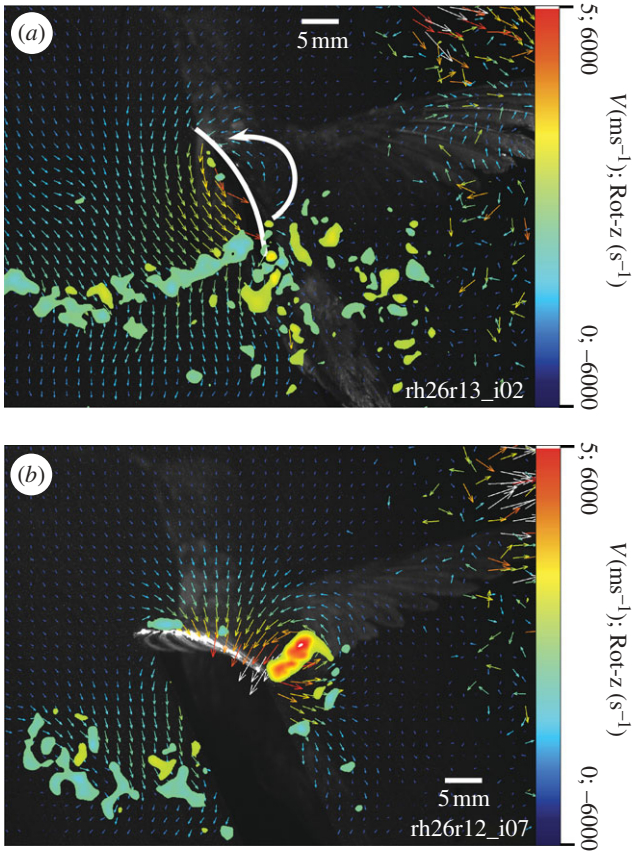

Figure 3. (*a*) The same *x*-section after upstroke translation has stopped (wing position 8). The pronating rotation of wing turn-around (large white arrow) has induced and sustained circulation around the wing (this image $|\Gamma_{\text{bound}}| = 0.08\ \text{m}^2\ \text{s}^{-1}$). (*b*) Beginning of downstroke translation (wing position 1). Note the shed upstroke/pronation vortex ($|\Gamma| = 0.08\ \text{m}^2\ \text{s}^{-1}$) behind the trailing edge, merged with the starting vortex of downstroke.

wake structure, was less than 2 per cent of peak ω in the vortex; a 10 per cent mask was applied to eliminate this background noise and allow definition of vortex structures. We integrated this vorticity with respect to area to arrive at circulation for the vortex. The strength of this dorsal, leading edge circulation was compared to the bound circulation on the wing ($\Gamma_{\text{LEV}}/\Gamma_{\text{bound}} \cdot 100$) as a percentage.

3. RESULTS

(a) *Bound and LEV circulation during translation*

The two-dimensional near-field sectional flow around hummingbird wings shows variable amounts of leading edge vorticity within 2 mm of the upper surface of the wing, but with no retrograde (i.e. towards the direction of wing translation) as described elsewhere for fruit flies, hawkmoths and dragonflies (Willmott *et al.* 1997; Birch *et al.* 2004; Bomphrey *et al.* 2005; figures 1*a* and 2*a*,*b*; see electronic supplementary material, figure 3). Circulation from summed vorticity on the upper surface of the wings during downstroke was far less than that measured for Γ_{bound}, ranging between 0.7 and 25.6 per cent (mean = 16%; see electronic supplementary material, figure 4) of Γ_{bound} (figures 3*a*,*b* and 4) and between 4.1 per cent and 14.1 per cent (mean = 7%) during upstroke. This dorsal vorticity is small compared with that measured in bats, where the summed vorticity on the upper surface of the wing represented 40 per cent of the circulation required for body support (Muijres *et al.* 2008).

Flow below the wing is highly influenced by suction around the sharp leading edge, with retrograde flows below the wings originating at approximately half-chord. The resulting bound circulation, measured using the line-integral method, during downstroke was in close agreement (4% greater) with our previously measured circulation calculated from summed vorticity shed into the far-field wake (Warrick *et al.* 2005), while the upstroke circulation here reported is 32 per cent greater than previously reported. This latter disparity may have been due to viscous decay and/or incomplete sampling of the weaker and more poorly defined upstroke tip vortex in the far-field wake. Nevertheless, our current study supports our earlier finding that the downstroke produces far greater aerodynamic force than the upstroke (mean downstroke circulation = 2.1 ± 0.1 × upstroke; $n = 5$ birds; difference between half-cycle circulation *t*-tests $p < 0.01$ for all birds), although the disparity was somewhat smaller that previously reported (approx. 3 times) (Warrick *et al.* 2005). Mindful of the uncertainties in calculating lift forces without directly measuring pressure distribution

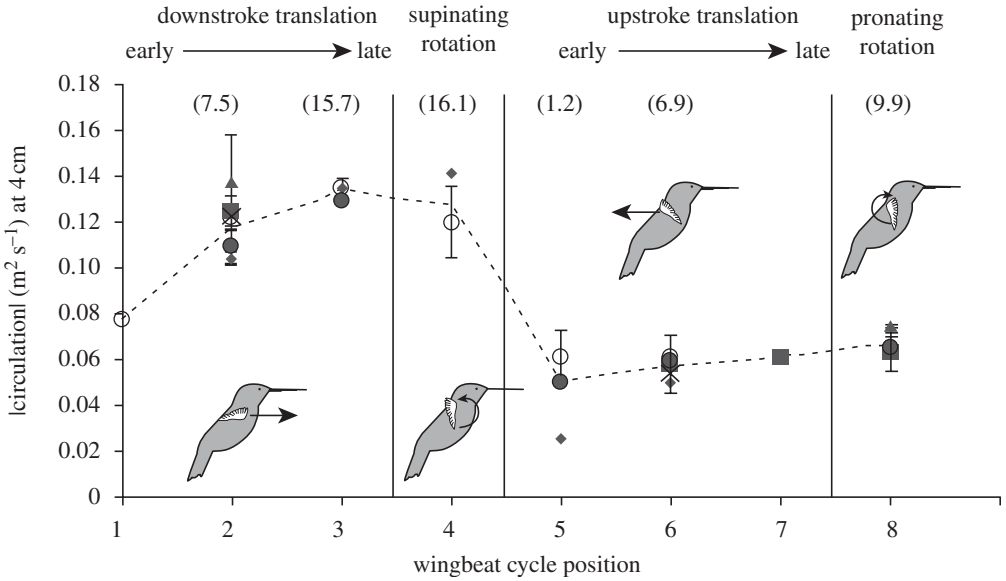

Figure 4. Absolute value of the bound circulation Γ_{bound} and circulation from leading-edge vorticity (Γ_{LEV}; in parentheses) around the 4 cm *x*-section throughout the wingbeat cycle. Not all birds were sampled at every position. Mid-downstroke circulation was significantly ($p \ll 0.05$) higher than mid-upstroke in all birds (rh20, d.f. = 5; rh23, d.f. = 4; rh26, d.f. = 3) for which both positions were measured. Birds sampled: ×, rh18; diamonds, rh22; triangles, rh23; vertical line through ×, rh25; solid circles, rh26; open circles, rh27.

(Dabiri 2005), the observed bound circulation (Γ_{bound}) at the 4 cm section through the wingbeat cycle provided an estimated 112 per cent of the lift needed for weight support (figure 3*a*).

(b) *Bound circulation during long-axis rotation*

Remarkably, the pattern of flow from the lower surface around the leading edge to the upper surface, continued well-beyond the end of half-cycle translation, and circulation during long-axis rotation (pronation, supination) was at least equal to that measured during the immediately preceding translation. Using the mean positional circulation for each bird, circulation during mid-to-late downstroke was statistically indistinguishable from that measured during supination (0.133 versus 0.131; $p = 0.44$; $n = 3$ and 2 birds, respectively), and circulation during mid-to-late upstroke was significantly lower than that during pronation (0.058 versus 0.067; $p = 0.04$; $n = 5$ and 3 birds, respectively). Overall, we estimate that a hovering hummingbird will experience only a brief (approx. 2 ms; 16% of wingbeat cycle) interruption in lift production as circulation is reversed at the beginning of each translation half-cycle.

4. DISCUSSION

(a) *The wake of a hovering hummingbird*

Our results help explain the far-field wake previously reported for hovering hummingbirds (Warrick *et al.* 2005; see electronic supplementary material, figures 5 and 6). Only after translational downstroke begins is the circulation from upstroke/pronation shed, with measured circulation in this shed vortex being indistinguishable from the bound circulation of upstroke/pronation measured an instant before (figure 4*b*). The far-field wake shows only one shed vortex produced at the upstroke/downstroke transition; the stopping vortex of upstroke and starting vortex of downstroke are so temporally and spatially close that they merge into one. In contrast, the vortex shed at the end of downstroke/supination is convected down by the greater downwash of downstroke, and this stopping vortex remains largely distinct from the starting vortex of upstroke (see electronic supplementary material, figures 5 and 6).

(b) *Bound and LEV circulation*

The LEV above a hummingbird wing is qualitatively different from that observed over the wings of a robotic fruitfly model ($Re = 120$; Birch & Dickinson 2001) and, perhaps, dragonflies ($Re = 4300$; Thomas *et al.* 2004) and hawkmoths ($Re = 5000$; Bomphrey *et al.* 2005), which all show stronger flow separation and retrograde or near-retrograde flow above the surface of the wing. Nevertheless, sharp leading edge aerodynamics still dictates flow over hummingbird wings. When the cross section of the aerofoil is thin and the angle of attack is high, the close proximity of the stagnation point to the high-velocity air from wing translation creates an extreme velocity and pressure gradient at the leading edge. In smaller insects, the resulting low pressure area at the leading edge is sufficient to produce retrograde flow and an attached vortex well above the leading edge of the wing. Our interpretation of the two-dimensional flow field over hummingbird wings is that the low pressure at the sharp leading edge (approx. 0.5 mm) of the wing strongly influences lift production by drawing air around from far beneath the ventral surface of the wing and creating a nearly laminar bound circulation able to almost completely circumscribe the small wing chord—a bound circulation we estimate to be more than sufficient for lift support.

Although we did not attempt to quantify spanwise flow, it is possible that a conical LEV, out-of-plane to our PIV images, spirals outward towards the wingtips as has been seen in the hawthmoth (Willmott *et al.* 1997). However, given the flow fields typical at the 4 cm slice

(figure 2*a*; electronic supplementary material, figure 3), our interpretation is that the flow field is dominated by the bound vortex, and that the vorticity on the upper surface of the wing has no structure independent of the bound vortex. Only three-dimensional PIV will fully resolve this issue.

Because 80+ per cent of the leading edge of a hummingbird wing is formed from the thin primary flight feathers (compared to 50–70% for other birds; Videler 2006), it is particularly suited to generating this type of flow. Interestingly, the leading edge of a swift wing is also largely (~70%; D. R. Warrick 1997, unpublished data) formed by the primaries, and leading edge vortices have been observed on models of their wings (Videler *et al.* 2004), although the flexed presentation of those wings makes comparisons with hummingbirds difficult. Nevertheless, data from spinning propellers emulating hummingbird wings (B. W. Tobalske and D. R. Warrick 2008, unpublished data) indicate that even a slight increase in leading edge thickness results in a dramatic reduction in lift, suggesting that minimizing the thick leading edge of the proximal wing is critical to the performance of hummingbird aerofoils.

(c) *Wing rotation*

The bound circulation on the hummingbird wing allows aerodynamic force production to continue through wing turnaround (figure 3*b*), with circulation maintained during long-axis wing rotation at the ends of the half cycles. How this force is used by the animal during hovering is unknown, but it is reasonable to hypothesize that this uninterrupted aerodynamic force production is a useful biomechanical resource with regard to weight support as well as control and stability during hovering.

There is no evidence from our results that long-axis rotation causes or augments bound circulation as it is hypothesized to do in insects (Dickinson *et al.* 1999; Lehmann 2004; figure 4*a*). While there is some evidence that pronation augments circulation at the end of the weaker upstroke (figure 4), we could find no evidence of 'starting' vorticity shed in the wake, as would be required if circulation were increased by wing rotation. Rather than a mechanism for creating additional bound circulation, then, the long-axis rotation used by hummingbirds may simply be sustaining bound circulation long enough to prevent vortex shedding at the end of translation, thus making wing turn-around as aerodynamically seamless as possible. Previous kinematic analyses indicate that this wing rotation occurs symmetrically between the end/beginning of the half strokes (Tobalske *et al.* 2007); that is, it is initiated slightly before the end of translation, and ends slightly after the beginning of the opposite translation. Thus, along with the apparent lack of wake shedding/re-capture and smooth transition from translational to rotational lift, much of wing turnaround may be free of the spiked peaks in lift production observed in robotic simulations of insect flight (Dickinson *et al.* 1999; Lehmann 2004), perhaps thereby facilitating the animal's ability to hold position at a nectar source.

In any case, the ability of a wing to rotationally induce and sustain bound circulation without vortex shedding may hinge on matching the geometry of the rotating chord to the geometry of the bound circulation; for a hummingbird, the rotation of the wing chord can occur within the same dimensions as the nearly-circular bound circulation from translation. This unique interaction between wings and air may help explain the wing-size paradox of hummingbirds: while committed to the most expensive form of flight (hovering; Tobalske *et al.* 2003), a flight regime where low wing loading should be favoured (Norberg & Rayner 1987), they posses relatively small wing area and average wing length (indicating small average wing chord; Greenwalt 1962). The flows observed here suggest that there may be dimensional restrictions for aerofoils able to exploit this mechanism, and studies of larger species may reveal the upper bounds of the aerodynamic grey area so deftly occupied by hummingbirds.

All procedures involving the animals were approved by the Institutional Animal Use and Care Committee at the University of Portland.

The authors thank Adrienne Nova and Matt Leineweber for their assistance in caring for hummingbirds and data collection. This research was supported by National Science Foundation grants IBN-0327380 and IOB-0615648S.

REFERENCES

Birch, J. M. & Dickinson, M. H. 2001 Spanwise flow and the attachment of the leading-edge vortex on insect wings. *Nature* **412**, 729–733. (doi:10.1038/35089071)

Birch, J. M., Dickson, W. B. & Dickinson, M. H. 2004 Force production and flow structure of the leading edge vortex on flapping wings at high and low Reynolds numbers. *J. Exp. Biol.* **207**, 1063–1072. (doi:10.1242/jeb.00848)

Bomphrey, R. J., Lawson, N. J., Harding, N. J., Taylor, G. K. & Thomas, A. L. R. 2005 The aerodynamics of *Manduca sexta*: digital particle image velocimetry analysis of the leading-edge vortex. *J. Exp. Biol.* **208**, 1079–1094. (doi:10.1242/jeb.01471)

Bomphrey, R. J., Lawson, N. J., Taylor, G. K. & Thomas, A. L. R. 2006 Application of digital particle image velocimetry to insect aerodynamics: measurement of the leading edge vortex and near wake of a Hawkmoth. *Exp. Fluids* **40**, 546–554. (doi:10.1007/s00348-005-0094-5)

Dabiri, J. O. 2005 On the estimation of swimming and flying forces from wake measurements. *J. Exp. Biol.* **208**, 3519–3532. (doi:10.1242/jeb.01813)

Dickinson, M. H., Lehmann, F. & Sane, S. P. 1999 Wing rotation and the aerodynamic basis of insect flight. *Science* **284**, 1954–1960. (doi:10.1126/science.284.5422.1954)

Ellington, C. P. 2006 Insects versus birds: the great divide. In *44th AIAA aerospace sciences meeting and exhibit*, vol. 35, pp. 1–6. Reston, VA: AIAA.

Ellington, C. P., Van Den Berg, C., Willmott, A. P. & Thomas, A. L. R. 1996 Leading-edge vortices in insect flight. *Nature* **384**, 626–630. (doi:10.1038/384626a0)

Finnemore, E. J. & Franzini, J. B. 2003 *Fluid mechanics with engineering applications*, 10th edn. Columbus, OH: McGraw-Hill.

Greenwalt, C. H. 1962 Dimensional relationships for flying animals. *Smithson. Misc. Coll.* **144**, 1–44.

Lehmann, F. O. 2004 The mechanisms of lift enhancement in insect flight. *Naturwissenschaften* **91**, 101–122. (doi:10.1007/s00114-004-0502-3)

Muijres, F. T., Johansson, L. C., Barfield, R., Wolf, M., Spedding, G. R. & Hedenström, A. 2008 Leading-edge vortex improves lift in slow-flying bats. *Science* **319**, 1250–1253. (doi:10.1126/science.1153019)

Norberg, U. M. & Rayner, J. M. V. 1987 Ecological morphology and flight in bats (Mammalia; Chiroptera): wing adaptations, flight performance, foraging strategy and echolocation. *Phil. Trans. R. Soc. Lond. B* **316**, 335–427. (doi:10.1098/rstb.1987.0030)

Raffel, M., Willert, C. & Kompenhans, J. 2002 *Particle image velocimetry: a practical guide*. Berlin, Germany: Springer.

Spedding, G. R., Hendenstrom, A. & Rosen, M. 2003*a* Quantitative studies of the wakes of freely flying birds in a low-turbulence wind tunnel. *Exp. Fluids* **34**, 291–303. (doi:10.1007/s00348-002-0559-8)

Spedding, G. R., Rosen, M. & Hedenstrom, A. 2003*b* A family of vortex wakes generated by a thrush in free flight in a wind tunnel of its entire natural range of flight speeds. *J. Exp. Biol.* **206**, 2313–2344. (doi:10.1242/jeb.00423)

Thomas, A. L. R., Taylor, G. K., Srygley, R. B., Nudds, R. L. & Bomphrey, R. J. 2004 Dragonfly flight: free-flight and tethered flow visualizations reveal a diverse array of unsteady lift-generating mechanisms, controlled primarily via angle of attack. *J. Exp. Biol.* **207**, 4299–4323. (doi:10.1242/jeb.01262)

Tobalske, B. W., Hedrick, T. L., Dial, K. P. & Biewener, A. A. 2003 Comparative power curves in bird flight. *Nature* **421**, 363–366. (doi:10.1038/nature01284)

Tobalske, B. W., Warrick, D. R., Clark, C. J., Powers, D. R., Hedrick, T. L., Hyder, G. A. & Biewener, A. A. 2007 Three-dimensional kinematics of hummingbird flight. *J. Exp. Biol.* **210**, 2368–2382. (doi:10.1242/jeb.005686)

Videler, J. J. 2006 *Avian flight*. Oxford ornithology series. Oxford, UK: Oxford University Press.

Videler, J. J., Stamhuis, E. J. & Povel, G. D. E. 2004 Leading edge vortex lifts swifts. *Science* **306**, 1960–1962. (doi:10.1126/science.1104682)

Warrick, D. R., Tobalske, B. W. & Powers, D. L. 2005 Aerodynamics of the hovering hummingbird. *Nature* **435**, 1094–1097. (doi:10.1038/nature03647)

Weis-Fogh, T. 1972 Energetics of hovering flight in hummingbirds and in *Drosophila*. *J. Exp. Biol.* **56**, 79–104.

Willmott, A. P., Ellington, C. P. & Thomas, A. L. R. 1997 Flow visualization and unsteady aerodynamics in the flight of the hawkmoth *Manduca sexta*. *Phil. Trans. R. Soc. Lond. B* **352**, 303–316. (doi:10.1098/rstb.1997.0022)